Advanced LPV-YK Control Design with Experimental Validation on Autonomous Vehicles

Hussam Atoui, Olivier Sename, Vicente Milanes, John Jairo Martinez Molina

Advanced LPV-YK Control Design with Experimental Validation on Autonomous Vehicles ⋆

Hussam Atoui [a,b], Olivier Sename [a], Vicente Milanes [c], John J. Martinez [a]

[a] *Univ. Grenoble Alpes, CNRS, Grenoble INP, GIPSA-lab, 38000 Grenoble, France*

[b] *Research Department, Renault SAS, 1 Avenue de Golf, 78280 Guyancourt, France*

[c] *Engineering Division, Renault España SA, Av. Madrid, 72, 47008 Valladolid, Spain*

Abstract

This paper presents and experimentally validates two new methodologies to perform a smooth switching between a set of Linear Parameter-Varying (LPV) controllers that have been designed separately for different objectives. For a given partition of the scheduling parameter region, a set of LPV controllers (polytopic and grid-based) are designed separately on each subregion based on Youla-Kucera (YK) parameterization. Such kind of parameterization is beneficial to switch or interpolate between multiple controllers without adding any constraints to the design of the local controllers and the switching signals. The closed-loop system is proved to guarantee stability and performance under arbitrary switching in terms of a set of Linear Matrix Inequalities (LMIs). An application to autonomous vehicle lateral control is chosen for its challenging objectives. Experimental validation and comparison are depicted to illustrate the performance improvement compared to previous LPV control approaches.

Key words: Linear parameter-varying system, Youla parameterization, Gain-scheduling, Switching control

1 Introduction

Linear Parameter-Varying (LPV) control techniques are widely used in different applications as in aerospace [18],[33], engine control [28], or autonomous vehicles [4], [5]. [17] presents . The synthesis of an LPV control can be formulated as a Linear Matrix Inequality (LMI) optimization problem using a single Lyapunov function, either quadratic [26] or parameter-dependent [35]. The main applied LPV approaches are: 1) Polytopic [3]; 2) Grid-based [34]; and 3) Linear Fractional Transformation (LFT) [2]. These LPV approaches have been compared and experimentally validated on a real automated vehicle in our previous work [7]. On the other hand, a single Lyapunov function for complex models with large parameter variations may not exist, or if it exists, it could be conservative.

The current paper aims to solve some of the main limitations of the polytopic and grid-based approaches, detailed later, based on Youla-Kucera (YK) interpolating/switching techniques. The interest behind YK concept is to parameterize a set of linear stabilizing controllers $K(Q)$ where each one is parameterized by its corresponding YK parameter Q [25]. This kind of configuration is structured by mapping a set of linear stabilizing controllers onto a Q-based controller. The following two sections discuss the limitations of both polytopic and grid-based approaches, and some solutions that are proposed in the literature.

1.1 Grid-based Approach

The grid-based approach uses a single parameter-dependent Lyapunov function to solve a set of parameter-dependent LMIs (pLMIs). Since a single parameter-dependent Lyapunov function could not be efficient for complex designs and large parameter regions, the first solution has been proposed in [24]. The objective is to design multiple LPV controllers based on multiple parameter-varying Lyapunov functions, each suitable for a specific parameter subregion, and switch between them to achieve better performance. The switching

⋆ Institute of Engineering Univ. Grenoble Alpes

Email addresses: hussam.atoui@renault.com (Hussam Atoui), olivier.sename@grenoble-inp.fr (Olivier Sename), vicente.milanes@renault.com (Vicente Milanes), john-jairo.martinez-molina@grenoble-inp.fr (John J. Martinez).

stability has been studied for hysteresis switching and switching with average dwell-time strategies. This methodology enhances the use of the switched LPV techniques in several applications, see for instance [9], [22], [27] ,[13].

On the other hand, it has been stated in [24] that the switched LPV controllers may not provide a smooth transient response during switching, where aggressive performance is obtained at switching instants. Such a case may lead to mechanical damage, decrease material lifetime, or signal saturation which is out of real application objectives. Following this work, several research studies have been involved in solving the switching smoothness. For instance, a bumpless transfer of switching controllers is proposed in [14] followed by some developments in [19], [12], and [31].

Finally, a smooth switching LPV controller has been proposed first in [15]. It is designed in considering adjustable interpolation functions and a higher order differential control signal. An iterative descent algorithm is applied to optimize three decision variables (the parameter-dependent Lyapunov functions, the local controllers, and the interpolation functions). It also augments the problem to two dimensional parameter regions. This concept is developed in the recent works [33] and [16], however, it increases the complexity and the design constraints of the local controllers to achieve their objectives.

1.2 Polytopic Approach

The polytopic approach is the most popular among the LPV control approaches. In many fields, especially aerospace, engineers are interested in applying the gain-scheduling method based on optimized designs at different operating points [10]. On the other hand, it is known to be the most conservative one [17]. One of the main causes is that the polytopic LPV synthesis requires a constant Lyapunov function to ensure quadratic stability, which increases the problem conservatism.

Moreover, the overbounding of the parameter set is considered as a main cause of conservatism. The operating region of the underlying LPV model is defined by a convex polytope containing the parameter trajectories. This convex parameter region may include vertices that are not attained by the real plant, resulting in conservatism. The reason is that the construction of the polytope is based on the assumption that all parameters vary independently, whereas they could be related to each other by inherent couplings. For example, the known bicycle model describing the lateral dynamics of an autonomous vehicle is parameterized by the scheduling parameters "v_x" and "$1/v_x$" [7] (being v_x the longitudinal speed). Such a situation might cause unstable models at the polytopic vertices. In addition, the parameters could be physically correlated with each other, such that some combinations of extreme values of the parameters do not occur in real operation. For example, an LPV model describing the vertical flight dynamics of an aeroplane might be parameterized by the external scheduling signals (i.e., parameters) "speed" and "altitude." But usually, the maximum speed is not reached for minimum altitude and vice versa [21].

Several solutions have been investigated in the literature to find a reduced convex parameter region. Several solutions has been investigated in the recent survey [23]. [8] suggests to construct convex polyhedrons along given parameter trajectories, and solve the control design problem using affine parameter-dependent LMIs. Unfortunately, these methods often result in a huge number of vertices or nonconvex parameter sets and thus in increased computational burden. Scheduling Dimension Reduction (SDR) approach is proposed in [21] which reduces the parameter set based on experimental data, and yields the benefit of tailoring a control design to specific trajectories. In [20], a Deep Neural Network (DNN) approach is used to develop the SDR methods and achieve higher model accuracy under scheduling dimension reduction. In [38] and [37], authors develop an LPV switching controller and prove its stability when switching among the overlapped subsets of a polytopic parameter region.

In [29], a YK configuration is proposed to improve the performance of a polytopic LPV control. On the other hand, [10] proposes a YK-based gain-scheduled controller by interpolating LTI controllers designed separately at the different vertices of a polytopic parameter region. The interpolation is performed as a function of the varying parameters of the LPV model. Closed-loop quadratic stability and performance are guaranteed at intermediate interpolation points of the convex domain. In [11], a fixed pole-assignment application is introduced using an LPV YK-based method to preserve the closed-loop poles at the same location by interpolating between different controllers. In addition, in our previous work [6], an LPV-YK control scheme has been proposed to interpolate between two LPV controllers, each one designed over a full polytopic region, to achieve multiple control performances. On the other hand, all the previous YK-based solutions are still conservative for systems having overbounding polytopic parameter region.

1.3 Motivation and Contribution

This paper proposes two advanced LPV-YK control approaches to improve the performance of the switched LPV controllers, with lower conservatism and design complexities. Among all the previous works which have shown successful and smooth LPV switching controllers as in [24], [12], and [15], all of them require the re-design of the local LPV controllers using proposed LMIs, de-

pending on the switching signals (e.g. hysteresis switching, switching with average dwell-time, etc.). It is worth mentioning that the re-design of all the local LPV controllers together may cause conservatism when increasing the number of subregions or parameter dimensions. The current paper proposes the YK parameterization to:

(1) Simplify the design of the LPV switching control system by decreasing the complexity of the LMI conditions (no need to re-design the local LPV controllers)
(2) Avoid any limitation on the switching signals without requiring constant Lyapunov function
(3) Smooth the control and state responses during the switching instants
(4) Avoid the re-design of the switching control scheme if one needs to add or remove any of the local LPV controllers as Plug&Play

The general contributions of this paper are:

- Design two new LPV-YK control structures, grid-based and partitioned polytopic-based LPV-YK controllers. Their main objective is to switch smoothly between local YK-based LPV controllers, each is designed to be suitable over a certain parameter sub-region. Their interest is to decrease the control design conservatism and limitations compared to the standard LPV control approaches, and improving the closed-loop performance.
- A switching scheme is drawn between multi-LPV controllers based on YK parameterization which guarantees the closed-loop stability and performance under arbitrary switching signals.
- The two proposed LPV-YK controllers are applied to lateral control of autonomous vehicles, on a real RENAULT ZOE automated car, with experimental validation and comparative analysis.

The paper is organized as follows: Section 2 designs the new grid-based LPV-YK concept with its stability proof. The partitioned polytopic-based LPV-YK control design with its stability proof is discussed in Section 3. Section 4 implements and experimentally validates both approaches on a real robotized RENAULT ZOE car. Finally, some concluding remarks are given in Section 5.

Notations in this paper are as follows. $\mathbb{I}[a,b]$ denotes the integer set from a to b. $\mathbb{R}$ stands for the set of real numbers. $\mathbb{R}^{m\times n}$ is the set of real $m\times n$ matrices. The transpose of a real matrix M is denoted by M^T. I and 0 denote an identity matrix and a zero matrix, respectively, of appropriate dimensions. $diag(X_1, X_2, ..., X_N)$ denotes a matrix with matrices X_1, X_2, ..., and X_N as diagonal blocks. In the whole paper, the subscript i of a system/matrix/variable of an LPV plant (e.g. $G(\rho)$) denotes the LPV system/matrix/variable of the plant when the varying-parameter $\rho \in \mathcal{P}_i$, where $\mathcal{P}_i$ is a subset of the full parameter region $\mathcal{P}$. In addition, the second subscript j γ_∞ corresponds to the known γ-performance design, whereas γ is a switching signal.

2 Grid-based LPV-YK control design

The following section aims to design a grid-based LPV-YK controller that switches between multiple LPV controllers, each suitable for a specific parameter region. The closed-loop system is proved to remain stable and its performance is optimized over the whole gridded parameter subregions. This approach improves the smooth LPV-switched control domain which has been already studied in the pioneering works [24], [15], [33], and [16].

2.1 LPV Plant and Controllers Description

Consider a Multi-Input-Multi-Output (MIMO) LPV system $G(\rho)$ with m inputs and p outputs:

$$G(\rho)\begin{cases}\dot{x}(t) = A(\rho(t))x(t) + B_1(\rho(t))w(t) + B_2(\rho(t))u(t)\\ z(t) = C_1(\rho(t))x(t) + D_{11}(\rho(t))w(t) + D_{12}(\rho(t))u(t)\\ y(t) = C_2(\rho(t))x(t) + D_{21}(\rho(t))w(t) + D_{22}(\rho(t))u(t)\end{cases} \tag{1}$$

where $x(t) \in \mathbb{R}^{n_x}$, $y(t) \in \mathbb{R}^p$, $u(t) \in \mathbb{R}^m$, $z(t) \in \mathbb{R}^{n_z}$ are the state, output, input, controlled output vectors respectively. $w(t) = \begin{bmatrix} r & n & d \end{bmatrix}^T \in \mathbb{R}^{n_w}$ contains the exogenous inputs of the tracking reference r, noise n and input disturbance d. All the state-space data are continuous functions of the parameter vector ρ. Assume that ρ is in a compact set $\mathcal{P} \subset \mathbb{R}^s$ with its parameter variation rate bounded by $\underline{\nu_k} \leq \dot{\rho}_k \leq \overline{\nu}_k$ for $k = 1, 2, ..., s$. Moreover, let us assume the following:

- $(A(\rho), B_2(\rho), C_2(\rho))$ triple is parameter-dependent stabilizable and detectable $\forall \rho \in \mathcal{P}$.
- $\begin{bmatrix} B_2^T(\rho) & D_{12}^T(\rho) \end{bmatrix}$ and $\begin{bmatrix} C_2(\rho) & D_{21}(\rho) \end{bmatrix}$ have full row ranks $\forall \rho \in \mathcal{P}$.
- $D_{22}(\rho) = 0$.

Suppose that the parameter set $\mathcal{P}$ is covered by a finite number of closed subsets $\{\mathcal{P}_i\}_{i\in Z_N}$, where the index set $Z_N = \{1, 2, \ldots, N\}$, and $\mathcal{P} = \bigcup \mathcal{P}_i$. At the boundaries between each adjacent subsets, there exist at least a single intersecting boundary or an intersecting surface.

Now, assume that
(A.3.1). *There exists an LPV output-feedback controller $K^{(0)}(\rho)$ which exponentially stabilizes $G(\rho)$ at the full parameter region $\mathcal{P}_0 := \mathcal{P}$. (following the approach in [35]),*
(A.3.2). *Over each parameter subset $\{\mathcal{P}_i\}_{i\in Z_N}$, there exists an LPV controller $K_i(\rho)$ pre-designed separately and exponentially stabilize $G(\rho)$ over $\{\mathcal{P}_i\}_{i\in Z_N}$. Each $K_i(\rho)$ is designed to achieve a suitable performance in its corresponding parameter region $\{\mathcal{P}_i\}_{i\in Z_N}$*

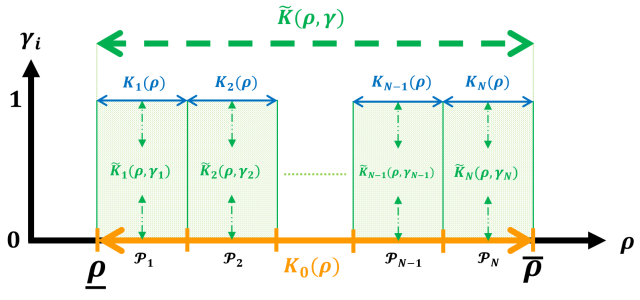

Fig. 1. LPV-YK gridded controller

The defined LPV controllers $K_i(\rho)$ $(i \geq 0)$ are described over $\mathcal{P}_i$ as

$$K_i(\rho) : \left[\begin{array}{c|c} A_{k,i}(\rho,\dot{\rho}) & B_{k,i}(\rho) \\ \hline C_{k,i}(\rho) & D_{k,i}(\rho) \end{array}\right] \quad , i \in \{0, Z_N\} \qquad (2)$$

where $A_{k,i}(\rho,\dot{\rho}) \in \mathbb{R}^{n_{k,i}\times n_{k,i}}$, $B_{k,i}(\rho) \in \mathbb{R}^{n_{k,i}\times m_k}$, $C_{k,i}(\rho) \in \mathbb{R}^{p_k\times n_{k,i}}$ and $D_{k,i}(\rho) \in \mathbb{R}^{p_k\times m_k}$. The closed-loop system performance is achieved in each parameter subregion and meanwhile maintains stability under any switching behavior via YK parameterization concept. The switching occurs when the parameter trajectory hits one of the subsets boundaries. In our proposed approach, the switching signal could be any continuous/discontinuous switching signal γ. The LPV closed-loop system for each pre-defined controller $K_i(\rho)$ over $\mathcal{P}_i$ can be described by

$$CL_i(\rho) : \left[\begin{array}{c|c} A_{cl,i}(\rho,\dot{\rho}) & B_{cl,i}(\rho) \\ \hline C_{cl,i}(\rho) & D_{cl,i}(\rho) \end{array}\right] \quad , i \in \{0, Z_N\} \qquad (3)$$

where $x_{cl,i}^T = \begin{bmatrix} x^T & x_{k,i}^T \end{bmatrix} \in \mathbb{R}^{n_x+n_{k,i}}$ $(i \geq 0)$. Notice that, for any $i \in \{0, Z_N\}$, the closed-loop system (3) is required to satisfy the bounded real lemma over $\mathcal{P}_i$ with a performance level $\gamma_{\infty,i}$, i.e. $\|z\|_2 < \gamma_{\infty,i}\|w\|_2$ and a symmetric, positive definite matrix functions $X_{cl,i}(\rho)$, each $X_{cl,i}(\rho)$ is smooth over its corresponding parameter subset $\mathcal{P}_i$, such that

$$\begin{bmatrix} \left\{ \begin{array}{c} A_{cl,i}^T(\rho)X_{cl,i}(\rho) + X_{cl,i}(\rho)A_{cl,i}(\rho) \\ + \sum_{k=1}^{s} \pm\{\underline{\nu}_k, \overline{\nu}_k\}\frac{\partial X_{cl,i}}{\partial \rho_k} \end{array} \right\} & X_{cl,i}(\rho)B_{cl,i}(\rho) & C_{cl,i}^T(\rho) \\ B_{cl,i}^T(\rho)X_{cl,i}(\rho) & -\gamma_{\infty,i}I_{n_w} & D_{cl,i}^T(\rho) \\ C_{cl,i}(\rho) & D_{cl,i}(\rho) & -\gamma_{\infty,i}I_{n_z} \end{bmatrix} < 0 \qquad (4)$$

2.2 Problem Definition

The objective of this work is to obtain exponential stability of the closed-loop system based on YK parameterisation. Moreover, a smooth interpolation scheme $\tilde{K}(\rho,\gamma)$ is formulated between multiple pre-designed LPV controllers $K_i(\rho)$ $(i \in Z_N)$, using the switching vector signal $\gamma = [\gamma_1, ..., \gamma_i, ..., \gamma_N]$, where each $K_i(\rho)$ is designed to be suitably used for a certain parameter subregion $\mathcal{P}_i$. This could be achieved by two steps:

(1) Parameterize each LPV controller $K_i(\rho)$ $(i \in Z_N)$ with respect to the nominal LPV controller $K_0(\rho)$, by an LPV-YK parameter $Q_i(\rho)$.
(2) At each boundary of two adjacent subsets $\mathcal{P}_i$ and $\mathcal{P}_{i+1}$, the interpolating signals γ_i and γ_{i+1} are adjusted in a way to switch from $K_i(\rho)$ to $K_{i+1}(\rho)$ or vise-versa. As a result, the overall parameterized LPV-YK controller $\tilde{K}(\rho,\gamma)$ stabilizes $G(\rho)$ $\forall\rho \in \mathcal{P}$ and for every continuous/discontinuous interpolating signals γ_i, $i \in Z_N$.

Figure 1 shows the partitioned parameter region $\mathcal{P}$ with intersecting boundaries. The orange solid line represents the chosen nominal LPV controller $K_0(\rho)$, as defined by assumption (A.3.1). The blue solid lines represent the local LPV controllers $K_i(\rho)$ $(i \in Z_N)$ as defined in assumption (A.3.2). The overall switching controller is performed using the interpolating signal $\gamma = [\gamma_1, ..., \gamma_N]$ $(\gamma_i \in [0, 1]\ \forall i)$, and is represented by the LPV-YK controller $\tilde{K}(\rho,\gamma)$.

2.3 Main Results

Based on the statements on LPV concepts and YK parameterization, the overall interpolation scheme which is referred to $\tilde{K}(\rho,\gamma)$ (see Fig. 4) is designed based on a Parametric Linear Matrix Inequality (PLMI) optimization problem, where its state-space matrices are represented as

$$\tilde{K}(\rho,\gamma) : \left[\begin{array}{c|c} \tilde{A}_k(\rho,\gamma) & \tilde{B}_k(\rho,\gamma) \\ \hline \tilde{C}_k(\rho,\gamma) & \tilde{D}_k(\rho,\gamma) \end{array}\right] \qquad (5)$$

being $\gamma(\rho)$ the vector of the parameter-dependent switching signals $\gamma_i(\rho)$ $(i \in Z_N)$ that are chosen here as follows:

- if $\gamma_i(\rho) = 0\ \forall i$, $\tilde{K}(\rho,\gamma) \equiv K_0(\rho)$.
- For any $\rho \in \mathcal{P}_m$, $\gamma_m(\rho) = 1$ and $\gamma_i(\rho) = 0$ $\forall i \neq m$, which implies that $\tilde{K}(\rho,\gamma)$ is equivalent to $\mathcal{F}_l(J(\rho), Q_m(\rho))$ that recovers $K_m(\rho)$ (refer to Fig. 4).

Lemma 2.1. *Assume that the matrices $A_{11}(\rho)$ and $A_{22}(\rho)$ are exponentially stable, every continuous and bounded block triangular matrix whose diagonal matrices consist of $A_{11}(\rho)$ and $A_{22}(\rho)$ is also exponentially stable.*

PROOF. Please see appendix A.

The following theorem aims to prove that $\tilde{K}(\rho,\gamma)$ exponentially stabilizes $G(\rho)$ for every $\rho \in \mathcal{P}$ and for every continuous/discontinuous switching signals γ_i.

Theorem 2.1. *Consider an LPV plant $G(\rho)$ (1), and that the assumptions (A.3.1) and (A.3.2) are satisfied. Let $K_0(\rho)$ be the nominal LPV controller designed over the full parameter region $\mathcal{P}_0$. Then, the parameterized LPV-YK controller $\tilde{K}(\rho,\gamma)$ (5)-(8) exponentially stabilizes $G(\rho)$, with an achieved performance $\|z\|_2 < \gamma_\infty \|w\|_2$, where $\gamma_\infty = \max\{\gamma_{\infty,i}\}_{i\in Z_N}$, for any continuous/discontinuous bounded switching signals $\gamma_i \in [0,1]$, if there exist symmetric, positive definite, parameter-dependent matrix functions $X_g(\rho) \in \mathbb{R}^{n_x \times n_x}$, $X_{k,0}(\rho) \in \mathbb{R}^{n_{k,0}\times n_{k,0}}$, and matrices $V(\rho)$ and $W(\rho)$ such that for any $\rho \in \mathcal{P}$:*

$$A(\rho)X_g(\rho) + X_g(\rho)A^T(\rho) + \sum_{j=1}^{s} \pm\{\underline{\nu}_j, \overline{\nu}_j\}\frac{\partial X_g}{\partial \rho_j} + B_2(\rho)V(\rho) + V^T(\rho)B_2^T(\rho) < 0 \tag{6}$$

$$A_{k,0}(\rho)X_{k,0}(\rho) + X_{k,0}(\rho)A_{k,0}^T(\rho) + \sum_{j=1}^{s} \pm\{\underline{\nu}_j, \overline{\nu}_j\}\frac{\partial X_{k,0}}{\partial \rho_j} + B_{k,0}(\rho)W(\rho) + W^T(\rho)B_{k,0}^T(\rho) < 0 \tag{7}$$

And $\forall \rho \in \mathcal{P}$, the state-space matrices of $\tilde{K}(\rho,\gamma)$ in (5) are

$$\tilde{A}_k(\rho,\gamma) = \begin{bmatrix} A(\rho) + B_2(\rho)F_g(\rho) - B_2(\rho)D_q(\rho,\gamma)C_2(\rho) & -B_2(\rho)D_q(\rho,\gamma)F_{k,0}(\rho) & B_2(\rho)C_q(\rho,\gamma) \\ -B_{k,0}(\rho)C_2(\rho) & A_{k,0}(\rho) & 0 \\ -B_q(\rho)C_2(\rho) & -B_q(\rho)F_{k,0}(\rho) & A_q(\rho) \end{bmatrix}$$

$$\tilde{B}_k(\rho,\gamma) = \begin{bmatrix} B_2(\rho)D_q(\rho,\gamma) & B_{k,0}(\rho) & B_q(\rho) \end{bmatrix}^T$$

$$\tilde{C}_k(\rho,\gamma) = \begin{bmatrix} F_g(\rho) - (D_{k,0}(\rho) + D_q(\rho,\gamma))C_2(\rho) & C_{k,0}(\rho) - D_q(\rho,\gamma)F_{k,0}(\rho) & C_q(\rho,\gamma) \end{bmatrix}$$

$$\tilde{D}_k(\rho,\gamma) = D_{k,0}(\rho) + D_q(\rho,\gamma) \tag{8}$$

where

$$\begin{aligned} A_q(\rho) &= diag(A_{q,1}, \ldots, A_{q,i}, \ldots, A_{q,N}), \\ B_q(\rho) &= \begin{bmatrix} B_{q,1} & \ldots & B_{q,i} & \ldots & B_{q,N} \end{bmatrix}^T, \\ C_q(\rho,\gamma) &= \begin{bmatrix} \gamma_1 C_{q,1} & \ldots & \gamma_i C_{q,i} & \ldots & \gamma_N C_{q,N} \end{bmatrix}, \\ D_q(\rho,\gamma) &= \sum_{i=1}^{N} \gamma_i D_{q,i} \end{aligned} \tag{9}$$

being $A_{q,i}$, $B_{q,i}$, $C_{q,i}$, and $D_{q,i}$ the state-space matrices of $Q_i(\rho)$ $\forall i \geq 1$ represented in (32), $F_g(\rho) = V(\rho)X_g^{-1}(\rho)$, and $F_{k,0}(\rho) = W_{k,0}(\rho)X_{k,0}^{-1}(\rho)$. Notice that $X_g^{-1}(\rho)$ and $X_{k,0}^{-1}(\rho)$ are chosen to be smooth over the whole parameter region $\mathcal{P}$.

PROOF.

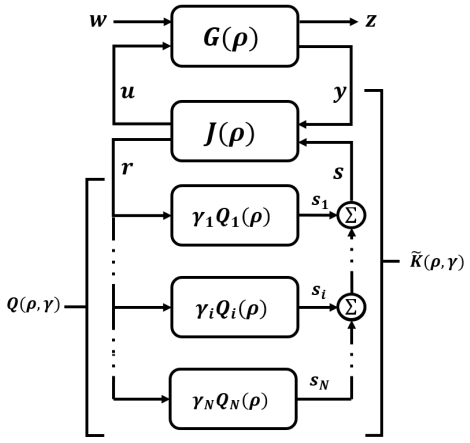

Fig. 2. Grid-based generalized LPV-YK configuration

According to YK concept, the parameterized controller can be formulated as a Linear Fractional Transformation (LFT) system [32], i.e. $\tilde{K}(\rho,\gamma) = \mathcal{F}_l(J(\rho), Q(\rho,\gamma))$ (see Fig. 4), where $J(\rho)$ is defined as:

$$J(\rho) = \left[\begin{array}{cc|cc} A(\rho) + B_2(\rho)F_g(\rho) & 0 & 0 & B_2(\rho) \\ -B_{k,0}(\rho)C_2(\rho) & A_{k,0}(\rho,\dot{\rho}) & B_{k,0}(\rho) & 0 \\ \hline F_g(\rho) - D_{k,0}(\rho)C_2(\rho) & C_{k,0}(\rho) & D_{k,0}(\rho) & I \\ -C_2(\rho) & -F_{k,0}(\rho) & I & 0 \end{array}\right] \tag{10}$$

and $Q(\rho,\gamma) = \sum_{i=1}^{N} \gamma_i(\rho)Q_i(\rho)$ (see $Q_i(\rho)$ in (32)). Specifically, a defined LPV controller $K_m(\rho)$ ($m \in [1,N]$) can be formulated as $\mathcal{F}_l(J(\rho), Q_m(\rho)))$, i.e. $K_m(\rho) \equiv \mathcal{F}_l(J(\rho), Q(\rho,\gamma))$ for $\gamma_m = 1$ and $\gamma_i = 0\ \forall i \neq m$

The following proof is achieved by two steps: 1) Prove that the LPV-YK parameter $Q(\rho,\gamma)$ is exponentially stable $\forall \rho \in \mathcal{P}$ and $\forall \gamma$; and 2) Prove the closed-loop exponential stability, $\forall \rho \in \mathcal{P}$, $\forall \gamma$, with γ_∞-performance level, where $\gamma_\infty = \max\{\gamma_{\infty,i}\}_{i\in Z_N}$.

Step 1:

Considering that (A.3.2) and (7) are satisfied,the triangular elements of $A_{q,i}(\rho)$ are shown to be exponentially stable $\forall \rho \in \{\mathcal{P}_i\}_{i\geq 1}$. Following **Lemma 2.1**, $A_{q,i}(\rho)$, consequently $Q_i(\rho)$, is exponentially stable over $\mathcal{P}_i$ $\forall i \geq 1$. As a result, $Q(\rho,\gamma) = \sum_{i=1}^{N} \gamma_i Q_i(\rho)$ is exponentially stable over $\mathcal{P} = \bigcup \mathcal{P}_i$ for every bounded signals $\gamma_i \in [0,1]$.

Step 2:

The LPV-YK closed-loop system $CL(\rho,\gamma)$ is derived from the LFT interconnection between $G(\rho)$ (1) and $\tilde{K}(\rho,\gamma)$ (8) (see Fig. 2). The closed-loop state matrix

$$Q_i(\rho) = \left[\begin{array}{cc:c:c} A(\rho)+B_2(\rho)D_{k,i}(\rho)C_2(\rho) & B_2(\rho)C_{k,i}(\rho) & B_2(\rho)[D_{k,i}(\rho)-D_{k,0}(\rho)]F_k - B_2(\rho)C_{k,0}(\rho) & B_2(\rho)[D_{k,i}(\rho)-D_{k,0}(\rho)] \\ B_{k,i}(\rho)C_2(\rho) & A_{k,i}(\rho,\dot\rho) & B_{k,i}(\rho)F_{k,0} & B_{k,i}(\rho) \\ \hdashline 0 & 0 & A_{k,0}(\rho)+B_{k,0}(\rho)F_{k,0}(\rho) & B_{k,0}(\rho) \\ \hline D_{k,i}^{(1)}C_2 - F_{g,i} & C_{k,i}(\rho) & [D_{k,i}(\rho)-D_{k,0}(\rho)]F_{k,0}(\rho) - C_{k,0}(\rho) & D_{k,i}(\rho)-D_{k,0}(\rho) \end{array}\right] \tag{11}$$

$A_{cl}(\rho,\gamma)$ is exponentially stable if $\forall\rho\in\mathcal{P}$, $\dot\rho\in[\underline{\nu},\overline{\nu}]$, there exists a symmetric, positive definite matrix function $X_{cl}(\rho)$ such that $\forall\gamma$:

$$A_{cl}^T(\rho,\gamma)X_{cl}(\rho) + X_{cl}(\rho)A_{cl}(\rho,\gamma) + \sum_{k=1}^{s}\dot\rho_k\frac{\partial X_{cl}}{\partial\rho_k} < 0 \tag{12}$$

Now , let $T = \begin{bmatrix} I & 0 & 0 & 0 \\ 0 & 0 & 0 & I \\ I & -I & 0 & 0 \\ 0 & 0 & I & 0 \end{bmatrix}$ be a state transformation matrix which is applied to $CL(\rho,\gamma)$ without changing its input-output nature, with $T^{-1} = \begin{bmatrix} I & 0 & 0 & 0 \\ I & 0 & -I & 0 \\ 0 & 0 & 0 & I \\ 0 & I & 0 & 0 \end{bmatrix}$.

Due to the block-triangular form of $\bar A_{cl}(\rho,\gamma)$ (13), (12) is satisfied if the following equations hold $\forall\rho\in\mathcal{P}$ (check **Lemma 2.1**):

$$Y_g(\rho)(A(\rho)+B_2(\rho)F_g(\rho))^T + (A(\rho)+B_2(\rho)F_g(\rho))Y_g(\rho) + \sum_{k=1}^{s}\dot\rho_k\frac{\partial Y_g}{\partial\rho_k} < 0 \tag{14a}$$

$$Y_q(\rho)A_q^T(\rho) + A_q(\rho)Y_q(\rho) + \sum_{k=1}^{s}\dot\rho_k\frac{\partial Y_q}{\partial\rho_k} < 0 \tag{14b}$$

$$A_{cl,0}^T(\rho)Y_{cl,0}(\rho) + Y_{cl,0}(\rho)A_{cl,0}(\rho) + \sum_{k=1}^{s}\dot\rho_k\frac{\partial Y_{cl,0}}{\partial\rho_k} < 0 \tag{14c}$$

where $Y_g(\rho)\in\mathbb{R}^{n_x\times n_x}$, $Y_q(\rho)\in\mathbb{R}^{n_q\times n_q}$ and $Y_{cl,0}(\rho)\in\mathbb{R}^{(n_x+n_{k,0})\times(n_x+n_{k,0})}$ are symmetric, positive definite matrix functions with $X_{cl}(\rho) = T^T\,\mathrm{diag}(Y_g, Y_q, Y_{cl,0})\,T$.

- Inequality (14a) can be deduced from (6) by choosing $Y_g(\rho) = X_g(\rho)$ and considering that $F_g(\rho) = V(\rho)X_g^{-1}(\rho)$ in (6).
- (14b) is satisfied since $Q(\rho,\gamma)$ has been proved in *Step 1* to be exponentially stable over $\mathcal{P}$.
- (14c) is fulfilled given that $K^{(0)}(\rho)$ exponentially stabilizes $G(\rho)$ according to (A.3.1).

Now, assume a sequence of finite switching time over the interval $[0,T]$ is $t_0, t_1, \ldots, t_N$ with $t_0 = 0$, knowing that the closed-loop Lyapunov function is $V(x_{cl}) = x_{cl}^T X_{cl}(\rho)x_{cl}$. From the YK basic concept [32], a parameterized controller $\tilde K = \mathcal{F}_l(J,Q)$ recovers the performance of its actual controller K. Thus, the closed-loop performance of $\mathcal{F}_l(G,\tilde K)$ is equivalent to the performance of $\mathcal{F}_l(G,K)$. In the current work, it can be deduced that the closed-loop performance of $CL(\rho,\gamma)$ is equivalent to that of $CL_i(\rho)$ (3) within each parameter subset $\mathcal{P}_i$. Notice that according to (4), the following inequality describes the performance of $CL_i(\rho)$ $\forall\rho\in\{\mathcal{P}_i\}_{i\in Z_N}$

$$\frac{d}{dt}(x_{cl,i}^T X_{cl,i}(\rho)x_{cl,i}) + \frac{1}{\gamma_{\infty,i}}z^Tz - \gamma_{\infty,i}w^Tw < 0 \tag{15}$$

On the other hand, it is worth mentioning that $X_{cl}(\rho)$ is independent of the switching signal γ, so, for any switching time t_k, $V(x_{cl}(t_k)) = V(x_{cl}(t_k^-))$, and thus

$$V(x_{cl}(t_k)) \le V(x_{cl}(t_k^-)) \tag{16}$$

Given the initial condition $x_{cl}(0) = 0$, from (15)-(16), it can be shown that the inequality

$$\dot V(x_{cl}) + \frac{1}{\gamma_\infty}z^Tz - \gamma_\infty w^Tw < 0, \quad \gamma_\infty = \max\{\gamma_{\infty,i}\}_{i\in Z_N} \tag{17}$$

holds within each parameter subset. Integrate on both sides, we get

$$V(x_{cl}(T)) - V(x_{cl}(0)) + \frac{1}{\gamma_\infty}\|z\|_2^2 - \gamma_\infty\|w\|_2^2 < 0$$

Since $V(x_{cl}(T)) \ge 0$ and $V(x_{cl}(0)) = 0$, $\|z\|_2 < \gamma_\infty\|w\|_2$ is achieved. Therefore, the closed-loop is exponentially stable with an achieved performance $\|z\|_2 < \gamma_\infty\|w\|_2$, where $\gamma_\infty = \max\{\gamma_{\infty,i}\}_{i\in Z_N}$.

$$\bar{A}_{cl}(\rho,\gamma) = TA_{cl}(\rho,\gamma)T^{-1} = \left[\begin{array}{cc:cc} A(\rho)+B_2(\rho)F_g(\rho) & B_2(\rho)C_q(\rho,\gamma) & -B_2(\rho)(F_g(\rho)-(D_{k,0}(\rho)+D_q(\rho,\gamma))C_2(\rho)) & B_2(\rho)(C_{k,0}(\rho)-D_q(\rho,\gamma)F_k(\rho)) \\ 0 & A_q(\rho,\dot{\rho}) & B_q(\rho)C_2(\rho) & -B_q(\rho)F_k(\rho) \\ \hdashline 0 & 0 & A(\rho)+B_2(\rho)D_{k,0}(\rho)C_2(\rho) & B_2(\rho)C_{k,0}(\rho) \\ 0 & 0 & B_{k,0}(\rho)C_2(\rho) & A_{k,0}(\rho,\dot{\rho}) \end{array}\right] \tag{13}$$

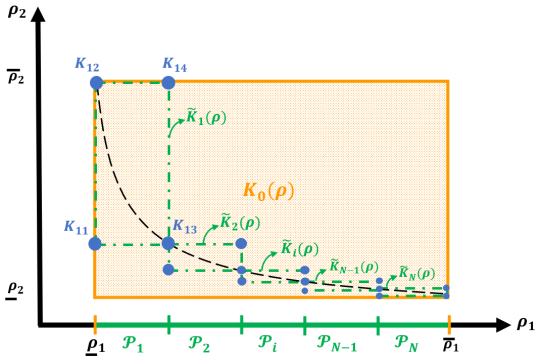

Fig. 3. Partitioned polytopic regions

3 Partitioned polytopic-based LPV-YK control design

This section presents an LPV-YK control scheme which: 1) formulates a YK-based gain-scheduling between LTI controllers that have been already designed separately at the polytopic vertices of each parameter subset; and 2) switches between the formulated gain-scheduling controllers over the partitioned polytopic subregions. The closed-loop system is proved to guarantee the quadratic stability for any continuous/discontinuous switching signals in terms of a set of Linear Matrix Inequalities (LMIs).

3.1 LPV Plant and Controllers Description

The following approach requires two model assumptions: 1) the system must be strictly proper ($D_{22}(\rho)=0$); and 2) the input and output matrices B_2, C_2, D_{12} and D_{21} must be parameter-independent [1]. From now on, we assume, without loss of generality, that the LPV system is given as:

$$G(\rho)\begin{cases} \dot{x}(t) = A(\rho)x(t)+B_1(\rho)w(t)+B_2u(t) \\ z(t) = C_1(\rho)x(t)+D_{11}(\rho)w(t)+D_{12}u(t) \\ y(t) = C_2x(t)+D_{21}w(t) \end{cases} \tag{18}$$

Notice that the second assumption doesn't impose any serious constraints since, if needed, it can be fulfilled by filtering the input u and output y (details are given in [3]).

Define $\mathcal{P}_0$ a convex polytope that contains all the parameter trajectories $\rho \in \mathbb{R}^{n_p}$. Let $\mathcal{P}_i$, $i \in Z_N = \{1,\dots,N\}$, be the convex polytopic subsets, that could intersect by a boundary or surface, defined in $\mathcal{P}_0$ along the parameter trajectories, i.e. $\rho \in \mathcal{P} = \bigcup_{i\geq 1}\mathcal{P}_i \subset \mathcal{P}_0$. Each $\mathcal{P}_i$ $(i \geq 0)$ is defined as:

$$\mathcal{P}_i := \mathcal{C}_{\mathcal{O}}\{w_{i1},...,w_{i2^{n_p}}\} \tag{19}$$

where w_{ij} represent the polytopic vertices of $\mathcal{P}_i$ $\forall j \in \mathbb{I}[1,2^{n_p}]$. ρ is then scheduled as:

$$\forall \rho \in \mathcal{P}_i, \quad \rho = \sum_{j=1}^{2^{n_p}} \alpha_{ij}(\rho)w_{ij}, \tag{20}$$

where $\forall i \sum_{j=1}^{2^{n_p}} \alpha_{ij}(\rho) = 1$, $\alpha_{ij}(\rho) \geq 0$ $\forall i,j$, being $\alpha_{ij}(\rho)$ the scheduling coefficients in the convex region $\mathcal{P}_i$.

Fig. 3 shows an example of a convex parameter region defined by two varying parameters $\rho_1 \in [\underline{\rho}_1, \overline{\rho}_1]$, and $\rho_2 \in [\underline{\rho}_2, \overline{\rho}_2]$, with $\rho_2 = 1/\rho_1$. The convex region $\mathcal{P}_0$ is represented in solid orange, and the convex subregions $\mathcal{P}_i$ $(i \geq 1)$ are bounded within dashed green polygons.

The LPV representation of $G(\rho)$ is defined over $\mathcal{P}_0$ as a convex combination of the state-space realizations of the local LTI systems G_{0j} at the vertices w_{0j}:

$$\left[\begin{array}{c|cc} A(\rho) & B_1(\rho) & B_2 \\ \hline C_1(\rho) & D_{11}(\rho) & D_{12} \\ C_2 & D_{21} & 0 \end{array}\right] = \sum_{j=1}^{2^{n_p}} \alpha_{0j}(\rho) \left[\begin{array}{c|cc} A_{0j} & B_{1,0j} & B_2 \\ \hline C_{1,0j} & D_{11,0j} & D_{12} \\ C_2 & D_{21} & 0 \end{array}\right] \tag{21}$$

Notice that $G(\rho)$ could be defined equivalently in terms of the LTI plants G_{ij} (at w_{ij}) as, for $\rho \in \mathcal{P}_i$:

$$\left[\begin{array}{c|cc} A(\rho) & B_1(\rho) & B_2 \\ \hline C_1(\rho) & D_{11}(\rho) & D_{12} \\ C_2 & D_{21} & 0 \end{array}\right] = \sum_{j=1}^{2^{n_p}} \alpha_{ij}(\rho) \left[\begin{array}{c|cc} A_{ij} & B_{1,ij} & B_2 \\ \hline C_{1,ij} & D_{11,ij} & D_{12} \\ C_2 & D_{21} & 0 \end{array}\right] \tag{22}$$

Now, assume that

(A.4.1). *There exists an LPV output-feedback controller $K_0(\rho)$ which quadratically stabilizes $G(\rho)$ (using the standard polytopic approach in [3]) over the full parameter*

region $\mathcal{P}_0$, defined as:

$$K_0(\rho): \left[\begin{array}{c|c} A_{k,0}(\rho) & B_{k,0}(\rho) \\ \hline C_{k,0}(\rho) & D_{k,0}(\rho) \end{array}\right] \tag{23}$$

being,

$$\left[\begin{array}{c|c} A_{k,0}(\rho) & B_{k,0}(\rho) \\ \hline C_{k,0}(\rho) & D_{k,0}(\rho) \end{array}\right] = \sum_{j=1}^{2^{n_p}} \alpha_{0j}(\rho) \left[\begin{array}{c|c} A_{k,0j} & B_{k,0j} \\ \hline C_{k,0j} & D_{k,0j} \end{array}\right] \tag{24}$$

where $A_{k,0}(\rho) \in \mathbb{R}^{n_{k,0}\times n_{k,0}}$, $B_{k,0}(\rho) \in \mathbb{R}^{n_{k,0}\times m_k}$, $C_{k,0}(\rho) \in \mathbb{R}^{p_k\times n_{k,0}}$ and $D_{k,0}(\rho) \in \mathbb{R}^{p_k\times m_k}$.

(A.4.2). *At each vertex w_{ij} ($j \in \mathbb{I}[1, 2^{n_p}]$, $i \geq 1$), a local LTI controller K_{ij} is designed separately to stabilize the local plant G_{ij}. It is worth mentioning that, at each intersecting boundary, a unique LTI controller should be designed at the intersecting extremums of the adjacent subsets respectively.*

Regarding the example in Fig. 3, the local LTI controllers at the intersecting boundaries w_{i3} and $w_{(i+1)2}$, $\forall i \in \mathbb{I}[1, N-1]$, are designed similarly. Consequently, the switching between two successive subsets ($\mathcal{P}_i$ and $\mathcal{P}_{i+1}$) undergoes using the same LTI controller ($K_{i3} \equiv K_{(i+1)2}$). In such a case, the state and control input energies,just before and just after switching, are not affected.

Fig. 3 represents an example of a convex parameter set partitioning. The dashed black curve represents the actual operating conditions of the parameters ($\rho_2 = 1/\rho_1$). The orange solid polygon represents the nominal LPV controller $K_0(\rho)$ designed using standard polytopic approach over the convex region $\mathcal{P}_0$. The blue points represent the local LTI controllers K_{ij} ($j \in \mathbb{I}[1, 4]$, $i \in \mathbb{I}[1, N]$) designed separately to stabilize G_{ij} at w_{ij} using any LTI control approaches. The green dashed polygons are the subsets chosen along the parameter trajectory. Over each subset $\mathcal{P}_i$, a gain-scheduled controller $\tilde{K}_i(\rho)$ is designed based on the YK interpolation of the local LTI controllers K_{ij}. The overall switching scheme between the $\tilde{K}_i(\rho)$ is represented by the LPV-YK controller $\tilde{K}_\sigma(\rho)$.

3.2 Problem Definition

The objective of this work is to:

(1) Design multiple YK-based gain-scheduled controllers $\tilde{K}_i(\rho)$, $i \in \mathbb{I}[1, N]$. Each one is designed by interpolating its corresponding LTI controllers K_{ij} ($j \in \mathbb{I}[1, 2^{n_p}]$) based on YK concept (refer to Fig. 3).
(2) Create an overall switched LPV-YK controller $\tilde{K}_\sigma(\rho)$ to switch between $\tilde{K}_i(\rho)$, such that $\tilde{K}_\sigma(\rho)$ quadratically stabilizes $G(\rho)$ $\forall \rho \in \mathcal{P}$ and for every continuous/discontinuous switching signal $\sigma(t)$. The switched closed-loop system is represented as

$$\tilde{CL}_\sigma(\rho): \left[\begin{array}{c|c} \tilde{A}_{cl,\sigma}(\rho) & \tilde{B}_{cl,\sigma}(\rho) \\ \hline \tilde{C}_{cl,\sigma}(\rho) & \tilde{D}_{cl,\sigma}(\rho) \end{array}\right] \tag{25}$$

3.3 Main Results

Based on the statements of LPV concepts and YK parameterization, the LPV-YK controllers $\tilde{K}_i(\rho)$ are designed based on a Linear Matrix Inequality (LMI) optimization problem, where they are defined as

$$\tilde{K}_i(\rho): \left[\begin{array}{c|c} \tilde{A}_{k,i}(\rho) & \tilde{B}_{k,i}(\rho) \\ \hline \tilde{C}_{k,i}(\rho) & \tilde{D}_{k,i}(\rho) \end{array}\right] \tag{26}$$

Lemma 3.1. *Consider a set of matrices A_i corresponding to each vertex of a convex hull $\mathcal{J} = \mathcal{C}_\mathcal{O}\{w_1, ..., w_{2^{n_p}}\}$, The following statements are equivalent:*

(i) A_i is Hurwitz $\forall i \in \mathbb{I}[1, 2^{n_p}]$
(ii) there exist 2^{n_p} transformation matrices Z_i such that the LPV matrix

$$\bar{A}(\rho) = \sum_{i=1}^{2^{n_p}} \alpha_i(\rho)\bar{A}_i = \sum_{i=1}^{2^{n_p}} \alpha_i(\rho) Z_i A_i Z_i^{-1} \tag{27}$$

is quadratically stable $\forall \rho \in \mathcal{J}$, where $\rho = \sum_{i=1}^{2^{n_p}} \alpha_i(\rho) w_i$ such that $\sum_{i=1}^{2^{n_p}} \alpha_i(\rho) = 1$, $\alpha_i(\rho) \geq 0$ $\forall i$.

Proof details are in [10].

Theorem 3.1. *Consider an LPV plant $G(\rho)$ (18), satisfying assumptions (A.3.1) and (A.3.2). Then, the switched LPV-YK controller $\tilde{K}_\sigma(\rho)$ (26)-(30) quadratically stabilizes $G(\rho)$ for any $\rho \in \mathcal{P}$ and for any continuous/discontinuous switching signals $\gamma_i \in [0, 1]$ ($\forall i \geq 1$), if there exist symmetric, positive definite, constant matrices $X_g \in \mathbb{R}^{n_x\times n_x}$, $X_{k,ij} \in \mathbb{R}^{n_{k,ij}\times n_{k,ij}}$, and matrices $W_j \in \mathbb{R}^{m\times n_x}$ and $V_{ij} \in \mathbb{R}^{m_k\times n_{k,ij}}$ such that:*

$$A_{0j}X_g + X_g A_{0j}^T + B_2 W_j + W_j^T B_2^T < 0 \quad \forall w_{0j} \tag{28}$$

$$A_{k,0}(w_{ij})X_{k,ij} + X_{k,ij}A_{k,0}^T(w_{ij}) + B_{k,0}(w_{ij})V_{ij} + V_{ij}^T B_{k,0}^T(w_{ij}) < 0 \quad \forall w_{ij} \tag{29}$$

with the state-space matrices of $\tilde{K}_i(\rho)$ are

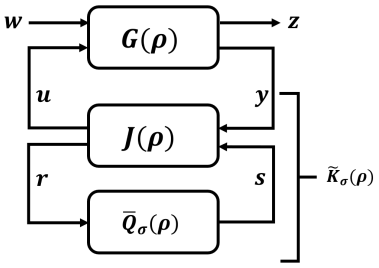

Fig. 4. Partitioned polytopic-based generalized LPV-YK configuration

$$\tilde{A}_{k,i}(\rho) = \sum_{j=1}^{2^{n_p}} \alpha_{ij}(\rho) \begin{bmatrix} A_{ij} + B_2 F_{g,ij} - B_2 \bar{D}_{q,ij} C_2 & -B_2 \bar{D}_{q,ij} F_{k,ij} & B_2 \bar{C}_{q,ij} \\ -B_{k,0}(w_{i,j}) C_2 & A_{k,0}(w_{i,j}) & 0 \\ -\bar{B}_{q,ij} C_2 & -\bar{B}_{q,ij} F_{k,ij} & \bar{A}_{q,ij} \end{bmatrix}$$

$$\tilde{B}_{k,i}(\rho) = \sum_{j=1}^{2^{n_p}} \alpha_{ij}(\rho) \begin{bmatrix} B_2 \bar{D}_{q,ij} & B_{k,0}(w_{i,j}) & \bar{B}_{q,ij} \end{bmatrix}$$

$$\tilde{C}_{k,i}(\rho) = \sum_{j=1}^{2^{n_p}} \alpha_{ij}(\rho) \begin{bmatrix} F_{g,ij} - (D_{k,ij} + D_{q,ij}) C_2 & C_{k,0}(w_{i,j}) - D_{q,ij} F_{k,ij} & \bar{C}_{q,ij} \end{bmatrix}$$

$$\tilde{D}_{k,i}(\rho) = \sum_{j=1}^{2^{n_p}} \alpha_{ij}(\rho) [D_{k,0}(w_{i,j}) + \bar{D}_{q,ij}] \tag{30}$$

$\forall i \in \mathbb{I}[1, N]$,

where $\bar{A}_{q,ij} = Z_{ij} A_{q,ij} (Z_{ij})^{-1}$, $\bar{B}_{q,ij} = Z_{ij} B_{q,ij}$, *and* $\bar{C}_{q,ij} = C_{q,ij} (Z_{ij})^{-1}$ $\forall i, j$, *and* Z_{ij} *are state transformation matrices chosen, to satisfy* ***Lemma 3.1****, such that* $\bar{A}_{q,i}(\rho) = \sum_{j=1}^{2^{n_p}} \alpha_j(\rho) Z_{ij} A_{q,ij} (Z_{ij})^{-1}$ *is quadratically stable* $\forall i \geq 1$. $A_{q,ij}$, $B_{q,ij}$, $C_{q,ij}$ *and* $D_{q,ij}$ *are the state-space matrices of* $Q_i(\rho)$ *(32) at the polytopic vertices* w_{ij}. *In addition,* $F_{g,j} = W_j X_g^{-1}$, $F_{k,ij} = V_{ij} (X_{k,ij})^{-1}$, *and* $F_{g,ij} = F_g(w_{ij})$.

PROOF. As mentioned in the previous proof, each parameterized controller can be formulated as a Linear Fractional Transformation (LFT) system [32]. Each LPV-YK controller can be written as $\tilde{K}_i(\rho) = \mathcal{F}_l(J(\rho), \bar{Q}_i(\rho))$ $\forall \rho \in \mathcal{P}_i$ (see Fig. 4), where $J(\rho)$ is represented in (10), and $\bar{Q}_i(\rho)$ is the transformed system of $Q_i(\rho)$ (32).

$$J(\rho) = \sum_{j=1}^{2^{n_p}} \alpha_i j(\rho) \left[\begin{array}{cc|cc} A_{ij} + B_2 F_{g,ij} & 0 & 0 & B_2 \\ -B_{k,0}(w_{ij}) C_2 & A_{k,0}(w_{ij}) & B_{k,0}(w_{ij}) & 0 \\ \hline F_{g,ij} - D_{k,0}(w_{ij}) C_2 & C_{k,0}(w_{ij}) & D_{k,0}(w_{ij}) & I \\ -C_2 & -F_{k,ij} & I & 0 \end{array}\right] \tag{31}$$

The following proof is achieved by two steps: 1) Prove that the LPV-YK parameter $\bar{Q}_i(\rho)$ is quadratically stable $\forall \rho \in \{\mathcal{P}_i\}_{i \in Z_N}$; and 2) Prove the closed-loop quadratic stability $\forall \rho \in \{\mathcal{P}_i\}_{i \in Z_N}$, $\forall \sigma$.

Step 1:

Knowing that: 1) K_{ij} stabilizes G_{ij} $\forall i \geq 1, \forall j \in [1, 2^{n_p}]$; and 2) (29) is satisfied, it can be shown that the triangular elements of $A_{q,ij}$ $\forall i, j$ are Hurwitz, and consequently, $A_{q,ij}$ is Hurwitz $\forall i, j$. According to **Lemma 3.1**, for any $i \geq 1$, there exist transformation matrices Z_{ij} such that the transformed system $\bar{Q}_i(\rho)$ is quadratically stable $\forall \rho \in \mathcal{P}_i$, choose $Z_{ij} = (X_{q,ij})^{1/2}$. As a result, $\bar{Q}_i(\rho)$ is quadratically stable $\forall \rho \in \mathcal{P}_i$.

3.4 Step 2:

The switched closed-loop system $CL_\sigma(\rho)$ is derived from the LFT interconnection between $G(\rho)$ and $\tilde{K}_\sigma(\rho)$ (see Fig. 4).

The switched closed-loop state matrix $A_{cl,\sigma}(\rho) = \sum_{j=1}^{2^{n_p}} \alpha_{\sigma j}(\rho) A_{cl,\sigma j}$ is quadratically stable if:

(1) There exist symmetric, positive definite, constant matrices $X_{cl,i}$ such that $\forall i \geq 1$

$$X_{cl,i} \tilde{A}_{cl,i}(\rho) + \tilde{A}_{cl,i}^T(\rho) X_{cl,i} < 0 \quad \forall \rho \in \mathcal{P}_i \tag{33}$$

(2) $\forall t_k \in [0, T]$, $V(x_{cl}(t_k)) \leq V(x_{cl}(t_k^-))$

Taking the same state transformation matrix T as in the previous proof, the transformed close-loop state matrix $\bar{A}_{cl,i}(\rho)$ is represented in (34). Due its block-triangular form, (12) is then satisfied if the following equations hold (check *Lemma 2* in [36]):

$$\sum_{j=1}^{2^{n_p}} \alpha_{ij}(\rho) (Y_{g,i}(A_{ij} + B_2 F_{g,ij}) + (A_{ij} + B_2 F_{g,ij})^T Y_{g,i}) < 0 \tag{35}$$

$$\sum_{j=1}^{2^{n_p}} \alpha_{ij}(\rho) (Y_{q,i} \bar{A}_{q,ij} + \bar{A}_{q,ij}^T Y_{q,i}) < 0 \tag{36}$$

$$Q_i(\rho) = \sum_{j=1}^{2^{n_p}} \alpha_{ij}(\rho) \left[\begin{array}{cc:c:c} A_{ij} + B_2 D_{k,ij} C_2 & B_2 C_{k,ij} & B_2[D_{k,ij} - D_{k,0}(w_{ij})]F_{k,ij} - B_2 C_{k,0}(w_{ij}) & B_2[D_{k,ij} - D_{k,0}(w_{ij})] \\ B_{k,ij} C_2 & A_{k,ij} & B_{k,ij} F_{k,ij} & B_{k,ij} \\ \hdashline 0 & 0 & A_{k,0}(w_i ij) + B_{k,0}(w_{ij}) F_{k,ij} & B_{k,0}(w_{ij}) \\ \hline D_{k,ij} C_2 - F_{g,ij} & C_{k,ij} & (D_{k,ij} - D_{k,0}(w_{ij}))F_{k,ij} - C_{k,0}(w_{ij}) & D_{k,ij} - D_{k,0}(w_{ij}) \end{array}\right] \tag{32}$$

$$\bar{A}_{cl,i}(\rho) = \sum_{j=1}^{2^{n_p}} \alpha_{ij}(\rho) T A_{cl,ij}(\gamma) T^{-1} = \sum_{i=1}^{2^{n_p}} \alpha_{ij}(\rho) \left[\begin{array}{cc:cc} A_{ij} + B_2 F_{g,ij} & B_2 \bar{C}_{q,ij} & -B_2(F_{g,ij} - (D_{k,0}(w_{ij}) + \bar{D}_{q,ij})C_2) & B_2(C_{k,0j}(w_{ij}) - \tilde{D}_{q,ij} F_{k,ij}) \\ 0 & \bar{A}_{q,ij} & \bar{B}_{q,ij} C_2 & -\bar{B}_{q,ij} F_{k,ij} \\ \hdashline 0 & 0 & A_{ij} + B_2 D_{k,0}(w_{ij}) C_2 & B_2 C_{k,0}(w_{ij}) \\ 0 & 0 & B_{k,0}(w_{ij}) C_2 & A_{k,0}(w_{ij}) \end{array}\right] \tag{34}$$

$$\sum_{j=1}^{2^{n_p}} \alpha_{ij}(\rho)(Y_i \mathcal{A}_{ij} + \mathcal{A}_{ij}^T Y_i) < 0 \tag{37}$$

where $Y_{g,i} \in \mathbb{R}^{n_x \times n_x}$, $Y_{q,i} \in \mathbb{R}^{n_q \times n_q}$ and $Y_i \in \mathbb{R}^{(n_x+n_{k,0})\times(n_x+n_{k,0})}$ are symmetric, positive definite, constant matrices, with $X_{cl,i} = T^T \operatorname{diag}(Y_{g,i}, Y_{q,i}, Y_i)\, T$, and

$$\mathcal{A}_{ij} = \begin{bmatrix} A_{ij} + B_2 D_{k,0}(w_{ij}) C_2 & B_2 C_{k,0}(w_{ij}) \\ B_{k,0}(w_{ij}) C_2 & A_{k,0}(w_{ij}) \end{bmatrix} \tag{38}$$

- Inequality (35) is equivalent to (28) by choosing $Y_{g,i} = X_g^{-1}$ and $W_j = F_{g,ij} X_g$ for every $\rho \in \mathcal{P}_i$.
- Since $\bar{Q}_i(\rho))$ is proved to be quadratically stable $\forall i$, inequality (36) is satisfied.
- (37) is fulfilled given that $K_0(\rho)$ quadratically stabilizes $G(\rho)$ over $\mathcal{P}_0$, and consequently over any $\mathcal{P}_i \subset \mathcal{P}_0$.

Therefore condition (33) is satisfied.

Assume a sequence of finite switching time over the interval $[0, T]$ is $t_0, t_1, \ldots, t_n$ with $t_0 = 0$, knowing that closed-loop Lyapunov function as $V(x_{cl}) = x_{cl}^T X_{cl,\sigma} x_{cl}$. From the YK basic concept, the closed-loop is written as $\mathcal{F}_l(G, J, Q)$. Consider a switching between any two adjacent subsets $\mathcal{P}_i$ and $\mathcal{P}_{i+1}$ $\forall i \geq 1$ at time t_k, then, the closed-loop dynamics switches from $\mathcal{F}_l(G, J_i, Q_{i,3})$ to $\mathcal{F}_l(G, J_i, Q_{i+1,2})$, or vise-versa. According to (A.4.2), $K_{i,3} \equiv K_{i+1,2}$ $\forall i \geq 1$, consequently $Q_{i,3} \equiv Q_{i+1,2}$. Then, for any switching time t_k, $\mathcal{F}_l(G, J, Q_{i,3}) = \mathcal{F}_l(G, J, Q_{i+1,2})$, and thus $V(x_{cl}(t_k)) = V(x_{cl}(t_k^-))$.

As a result, the switched closed-loop system $CL_\sigma(\rho)$ is quadratically stable $\forall \rho \in \mathcal{P}$, and for any continuous/discontinuous switching signal σ.

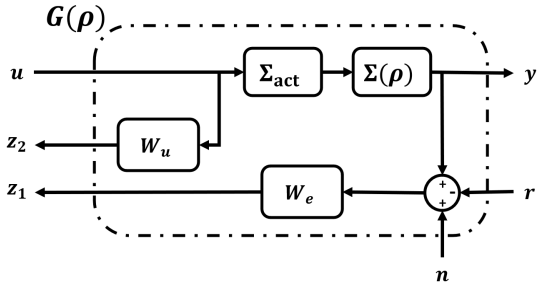

Fig. 5. Generalized plant $G(\rho)$

4 Application to Autonomous Vehicles

The proposed method is applied to the lateral dynamics of an autonomous vehicle, since it contains a non-affine scheduling parameter which causes an overbounding convex parameter region when implementing the polytopic approach. Recently, the polytopic, grid-based, and LFT approaches has been experimentally validated for lateral control of an automated vehicle in [7]. The lateral bicycle model is chosen, and taking into consideration the steering actuator dynamics.

4.1 Modelling Step

In [7], the lateral bicycle model $\Sigma(\rho)$ has been formulated for gridded and convex parameter regions. The longitudinal speed v_x is the varying parameter that varies in $[5, 30]$ m/s. For the gridded parameter region, the state-space representation of $\Sigma(\rho)$ is written as:

$$\Sigma(\rho) \begin{cases} \dot{x}(t) = A_\Sigma(\rho) x(t) + B_\Sigma u(t) \\ y(t) = C_\Sigma x(t) \end{cases} \tag{39}$$

being

$$x(t) = \begin{bmatrix} v_y \\ w \end{bmatrix},\ u(t) = \delta,\ B_\Sigma = \begin{bmatrix} \frac{C_f}{m} \\ \frac{C_f l_f}{I} \end{bmatrix},\ C_\Sigma = \begin{bmatrix} 0 & 1 \end{bmatrix},$$

$$A_\Sigma(\rho) = \begin{bmatrix} -\frac{C_r+C_f}{m\rho} & -\frac{C_f l_f - C_r l_r}{m\rho} - \rho \\ -\frac{C_f l_f - l_r C_r}{I\rho} & -\frac{C_f l_f^2 + l_r^2 C_r}{I\rho} \end{bmatrix}, \tag{40}$$

where v_y and w are the lateral and rotational velocities in the vehicle's frame, respectively. δ is the control input, the steering angle of the front tire. C_f and C_r represent the stiffness of the front and rear wheel-tires. I, m, l_f and l_r are the vehicle's inertia, mass and the distance from the center of gravity to the front and rear wheel axes respectively.

On the other hand, to represent $\Sigma(\rho)$ in a convex parameter region, the parameter-varying state-space matrices (i.e. $A_\Sigma(\rho)$) should be written in affine parameter-dependency as:

$$A_\Sigma(\rho) = \begin{bmatrix} -\frac{C_r+C_f}{m}\rho_2 & -\frac{C_f l_f - C_r l_r}{m}\rho_2 - \rho_1 \\ -\frac{C_f l_f - l_r C_r}{I}\rho_2 & -\frac{C_f l_f^2 + l_r^2 C_r}{I}\rho_2 \end{bmatrix}, \tag{41}$$

with $\rho_1 = v_x$ and $\rho_2 = \frac{1}{v_x}$. Notice that, in the coming control designs, (40) is used for the gridded parameter regions and (41) is used for convex parameter regions. Notice that the bicycle model is extended by considering an identified steering actuator dynamics Σ_{act}.

4.2 Lateral Control Design

In this work, the LPV and LTI controllers are designed using the $\mathcal{H}_\infty$ concept. For control design purpose, two weighting transfer functions $W_e(s)$ and $W_u(s)$ are designed to present the tracking performance and the actuator limitations respectively. Then, the state-space representation of $G(\rho)$ is obtained from the generalized plant shown in Fig. 5.

The longitudinal speed is assumed to vary within the range $\rho \in \mathcal{P} = [5, 30]\ m/s$, with a variation $\dot{\rho} \leq 5\ m/s^2$. Since the system dynamics changes significantly in this speed range, it could be conservative to design a single LPV controller over the full parameter region. Thus, the parameter region is divided into 5 subsets as:

$$\rho \in [5, 10] \cup [10, 15] \cup [15, 20] \cup [20, 25] \cup [25, 30] \tag{42}$$

Consider the following weighting functions to be used in the control design:

$$W_{e,0}(s) = \tfrac{s+2}{2s+0.002},\ W_{u,0}(s) = \tfrac{s+5}{0.01s+5} \tag{43}$$

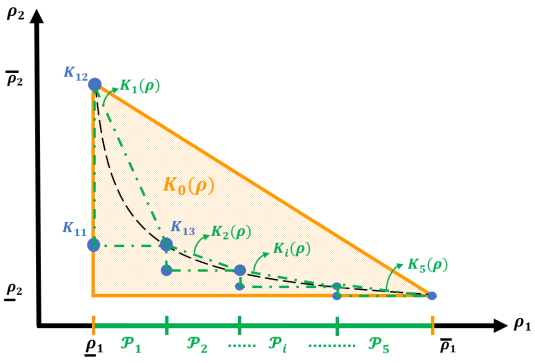

Fig. 6. Partitioned parameter region

$$W_e(s) = \tfrac{s+2}{2s+0.002},\ W_u(s) = \tfrac{s+10}{0.01s+10} \tag{44}$$

4.2.1 Grid-based control design

This section designs the proposed grid-based LPV-YK controller accordingly to the next steps:

- The nominal controller $K_0(\rho)$ is designed using $W_{e,0}$ and $W_{u,0}$ over the full parameter region $\mathcal{P}$ satisfying (A.3.1). Following (A.3.2), the controllers $K_i(\rho)$ are designed separately over $\mathcal{P}_i$ ($i \in [1, 5]$), with the same weighting functions W_e and W_e.
- Following the conditions of **Theorem 2.1**, the LPV state-feedback gains $F_g(\rho)$ and $F_{k,0}(\rho)$ are designed using the LMIs (6)-(7), where the multiple parameter-dependent Lyapunov functions at each subset are specified as affine and smooth functions of scheduling parameters. That is,

$$X_g(\rho) = X_g^0 + X_g^1\ \rho,\quad X_{k,0}(\rho) = X_{k,0}^0 + X_{k,0}^1\ \rho,$$

  where matrices X_g^j and $X_{k,0}^j$, $j = 0, 1$ are the optimization variables to be determined.
- $J(\rho)$ and $Q_i(\rho)$ ($i \in [1, 5]$) are obtained from (10)-(32).
- $Q(\rho, \gamma) = \sum_{i=1}^{5} \gamma_i(\rho) Q_i(\rho)$, where $\gamma_i(\rho)$ is switched between {0,1} when $\rho(t)$ touches the switching instants. Then, the LPV-YK controller $\tilde{K}(\rho, \gamma)$ is ready to be implemented.

4.2.2 Partitioned polytopic-based control design

In this section, $G(\rho)$ is written as a convex combination of the vertices of a triangular polytope $\mathcal{P}^{(0)} = \mathcal{CO}\{(\underline{\rho_1}, \underline{\rho_2}), (\underline{\rho_1}, \overline{\rho_2}), (\overline{\rho_1}, \underline{\rho_2})\}$ as shown in Fig. 6. The following section aims to design proposed partitioned polytopic-based LPV-YK control. Five triangular convex subsets ($\mathcal{P}_1 \ldots \mathcal{P}_5$) are chosen along the parameter trajectory as shown in Fig. 6. At the polytopic vertices

w_{ij} $\forall i \in \mathbb{I}[1,3], \forall j \in \mathbb{I}[1,5]$, LTI controllers K_{ij} are designed separately using the same weighting functions W_e and W_u. In addition, a polytopic LPV controller $K_0(\rho)$ is designed, based on (A.4.1), using $W_{e,0}$ and $W_{u,0}$.

For the partitioned polytopic-based LPV-YK control design, the following steps are done:

- According to the method explained in Section 3.3, the LPV polytopic-based state-feedback controller $F_g(\rho)$, and the LTI state-feedback controllers $F_{k,i}^{(0)}$, $\forall i \in \mathbb{I}[1,4]$, can be designed using an LMI-based state-feedback approach (pole-placement constraints or Linear Quadratic Regulator).
- $J(\rho)$ and $\tilde{Q}(\rho,\gamma)$ are obtained from (31)-(32) and as mentioned in the proof of **Theorem 3.1**.

As a result the partitioned polytopic-based LPV-YK control scheme $\tilde{K}_\sigma(\rho)$ is designed, and σ switches when ρ hits the subsets boundaries.

4.3 Experimental Results

The experiments shown here have been carried out on a robotized electric Renault ZOE vehicle shown in Fig. 7. It is prepared for lateral and longitudinal controls by computer-controlled steering and pedal actuators. Vehicle speed and the global coordinates are measurable using GPS and IMU. The vehicle is employed using a dSPACE MicroAutoBox. The test results of the designed controllers are discussed concerning their implementation and the analysis of the obtained performance.

In addition to the grid-based and partitioned polytopic-based LPV-YK controllers, two more controllers are tested for comparison purpose: 1) LPV-switched controller designed using the Theorem presented in [24]; and 2) A gain-scheduled LPV-YK controller that is designed by interpolating the LTI controllers at the vertices of $\mathcal{P}_0$, as presented in [12]. These two controllers are chosen to compare and show the improvement of our proposed approaches. The tests are done in a private test track in *Satory* (France) as shown in Fig. 8. This track contains bad road conditions and road-inclinations which allows to evaluate the controller robustness. The first part of the test describes the response of the controllers at a straight highway with high speeds. The second part concerns the precision of lateral control at optimal speeds chosen coherently depending on the road curvature. The longitudinal speed is considered as an external parameter of the LPV mode that is shown in Fig. 9. Fig. 10 presents the operating parameter subset that switches according to the speed evolution.

In the next two subsections, the vehicle performance is analyzed and compared between the grid-based LPV-YK controller and the LPV-switched controller [24], and

Fig. 7. Renault ZOE automated vehicle

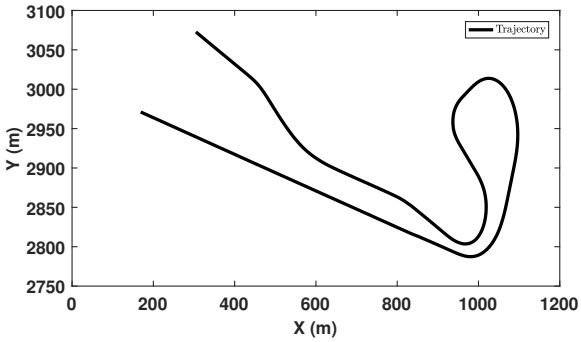

Fig. 8. Experimental planned and controlled trajectories

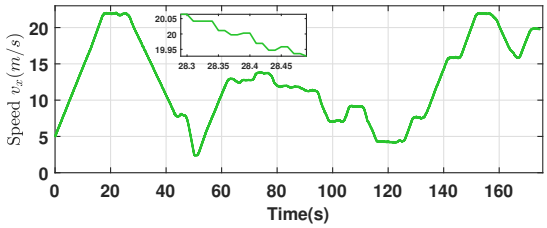

Fig. 9. Experimental longitudinal speed v_x (Kph)

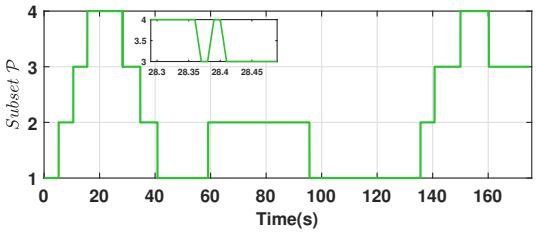

Fig. 10. Parameter subsets

between the partitioned polytopic-based LPV-YK controller and the gain-scheduled LPV-YK controller. Notice that, in all the tests, a restarting mode of the navigation systems appears at the end of the highway. Consequently, the results analysis doesn't concern the boarded part marked "NAV".

4.3.1 Grid-based LPV-YK control

Fig. 11a shows that both controllers achieve minimized lateral error. However, Fig. 11b and 11c emphasize a

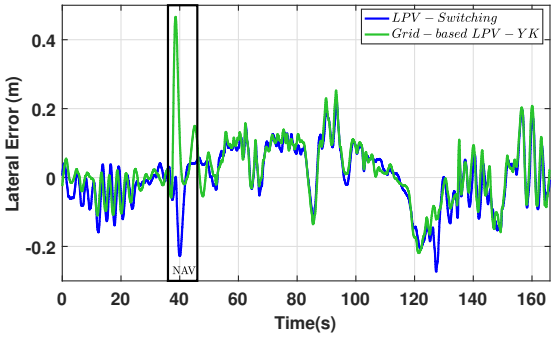

(a) Lateral error y_e (m)

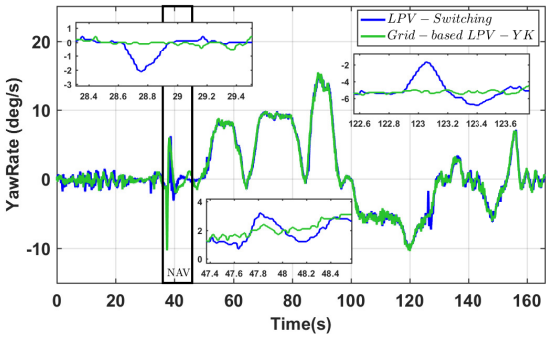

(b) Yaw rate w (deg/s)

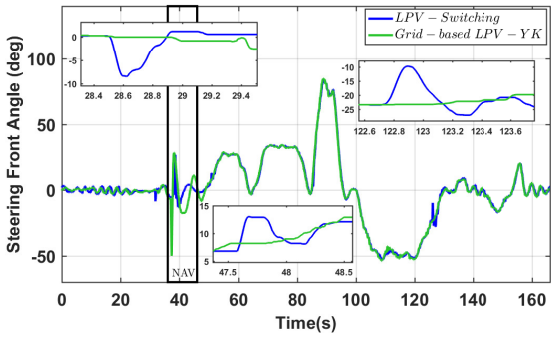

(c) Steering front angle δ (deg)

Fig. 11. Grid-based LPV-YK control

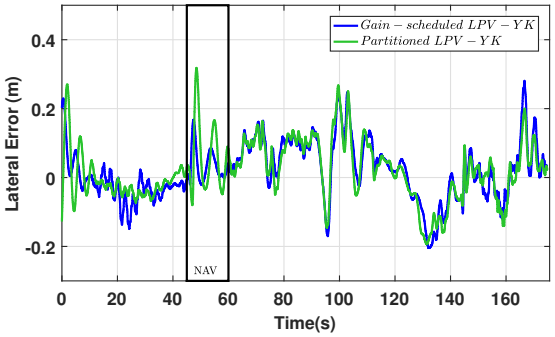

(a) Lateral error y_e (m)

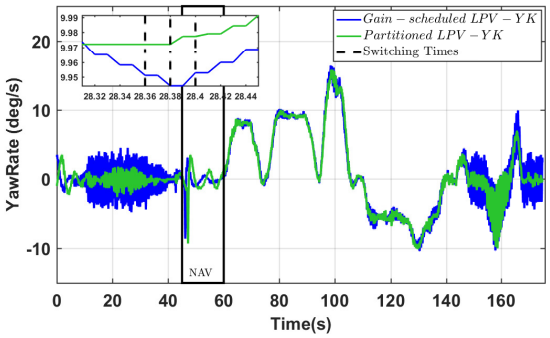

(b) Yaw rate w (deg/s)

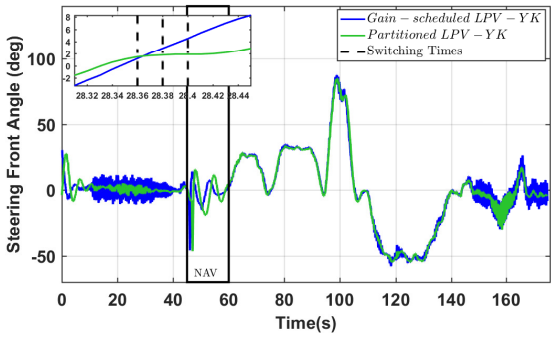

(c) Steering front angle δ (deg)

Fig. 12. Partitioned polytopic-based LPV-YK control

clear difference in performances during switching from one subset to another. The zoomed parts in Fig. 11c show that the switching effect is negligible using the proposed grid-based LPV-YK controller, which is not the case for the switched LPV controller.

Moreover, it is worth mentioning that the control input response at high speeds is not noisy. However, it has been shown previously that designing a single LPV grid-based controller over the whole parameter region could cause noisy performance at high speed as discussed in [7].

4.3.2 Partitioned polytopic-based LPV-YK control

It is shown in Fig. 12a that both controllers, the proposed partitioned and gain-scheduled LPV-YK, could successfully achieve lateral error minimization. On the other hand, the gain-scheduled LPV-YK controller leads to higher steering oscillations, compared to the partitioned LPV-YK controller, as shown in Figs. 12b and 12c. When $t \in [28.3, 28.5]s$, it is observed in Fig. 10 switches hysterically back and forth between the subsets $\mathcal{P}^{(3)}$ and $\mathcal{P}^{(4)}$. However, the hysterical switching of the partitioned LPV-YK controller between both subsets didn't affect the performance of the steering input and consequently the yaw rate (see the zoomed part in Figs. 12c and 12b). This is expected since,

at that instants, the operating controllers at that intersecting boundary are dynamically equivalent, i.e. $\mathcal{F}_l(G, J_{33}, Q_{33}) \equiv \mathcal{F}_l(G, J_{42}, Q_{42})$.

5 Conclusion

This work has proposed advanced LPV-YK switching methods to obtain smooth switching between parameter subregions. The switching signal is parameter-dependent which can be any continuous/discontinuous signal. The main advantages behind these approaches, compared to the previous LPV-switched controllers are: 1) The pre-designed LPV controllers are parameterized with respect to a nominal LPV controller, instead of requiring the redesign in new constrained LMIs; 2) The design conditions proposed for LPV-YK switching control are more smooth and can be satisfied assuming the LPV stabilizability of the system; 3) The local controllers can be designed using different control approaches, i.e. PID, $\mathcal{H}_\infty$, etc; and finally 4) The proposed LPV-YK control schemes doesn't pose any conditions or limitations on the switching signals.

As a future work, an interest appears to study the choice of Q dynamics, i.e. how to choose the best design of the state-feedback gains F_g and $F_{k,0}$, and how they affect the closed-loop performance.

Acknowledgements

Authors express their gratitude to RENAULT research department for its support in developing experimental tests. Special thanks to Alexendre ARMAND who helped in achieving the experimental results. This paper reflects solely the views of the authors and not necessarily the views of the company they belong to.

References

[1] G.Z. Angelis. *System analysis, modelling and control with polytopic linear models*. PhD thesis, Department of Mechanical Engineering, 2001.

[2] P. Apkarian and P. Gahinet. A convex characterization of gain-scheduled H_∞ controllers. *IEEE Transactions on Automatic Control*, 40(5):853–864, May 1995.

[3] P. Apkarian, P. Gahinet, and G. Becker. Self-scheduled h control of linear parameter-varying systems: a design example. *Automatica*, 31(9):1251–1261, 1995.

[4] H. Atoui, V Milanés, O. Sename, and John J Martinez. Design And Experimental Validation Of A Lateral LPV Control Of Autonomous Vehicles. In *23rd International Conference on Intelligent Transportation Systems (ITSC)*, Virtual Conference, Greece, September 2020.

[5] H. Atoui, O. Sename, E. Alcala, and V. Puig. Parameter Varying Approach For A Combined (Kinematic + Dynamic) Model Of Autonomous Vehicles. In *21st IFAC World Congress*, Berlin, Germany, July 2020.

[6] Hussam Atoui, Olivier Sename, Vicente Milanes, and John J. Martinez. Interpolation of multi-lpv control systems based on youla–kucera parameterization. *Automatica*, 134:109963, 2021.

[7] Hussam Atoui, Olivier Sename, Vicente Milanés, and John Jairo Martinez. LPV-Based Autonomous Vehicle Lateral Controllers: A Comparative Analysis. *IEEE Transactions on Intelligent Transportation Systems*, pages 1–12, 2021.

[8] T. Azuma, R. Watanabe, K. Uchida, and M. Fujita. A new lmi approach to analysis of linear systems depending on scheduling parameter in polynomial forms. 48(4):199–199, 2000.

[9] Bei Lu, Fen Wu, and SungWan Kim. Switching lpv control of an f-16 aircraft via controller state reset. *IEEE Transactions on Control Systems Technology*, 14(2):267–277, 2006.

[10] F. Bianchi and R.S. Peña. Interpolation for gain-scheduled control with guarantees. *Automatica*, 47(1):239–243, 2011.

[11] F. Blanchini, D. Casagrande, S. Miani, and U. Viaro. Stable lpv realization of parametric transfer functions and its application to gain-scheduling control design. *IEEE Transactions on Automatic Control*, 55(10):2271–2281, Oct 2010.

[12] Pang-Chia Chen, Sun-Li Wu, and Hung-Shiang Chuang. The smooth switching control for tora system via lmis. In *IEEE ICCA 2010*, pages 1338–1343, 2010.

[13] P. H. Colmegna, R. S. Sánchez-Peña, R. Gondhalekar, E. Dassau, and F. J. Doyle. Switched lpv glucose control in type 1 diabetes. *IEEE Transactions on Biomedical Engineering*, 63(6):1192–1200, 2016.

[14] Jan Dimon, Bendtsen Jakob, and Klaus Trangbaek. Bumpless transfer between observer-based gain scheduled controllers. *International Journal of Control*, 78, 01 2005.

[15] Masih Hanifzadegan and R. Nagamune. Smooth switching lpv controller design for lpv systems. *Automatica*, 50:1481–1488, 2014.

[16] Tianyi He, Guoming Zhu, and Sean Swei. Smooth switching lpv dynamic output-feedback control. *International Journal of Control, Automation and Systems*, 18:1367–1377, 12 2019.

[17] C. Hoffmann and H. Werner. A survey of linear parameter-varying control applications validated by experiments or high-fidelity simulations. *IEEE Transactions on Control Systems Technology*, 23(2):416–433, March 2015.

[18] Weilai Jiang, Kangsheng Wu, Zhaolei Wang, and Yaonan Wang. Gain-scheduled control for morphing aircraft via switching polytopic linear parameter-varying systems. *Aerospace Science and Technology*, 107:106242, 2020.

[19] Michel Kinnaert, Thomas Delwiche, and Joseph Yamé. State resetting for bumpless switching in supervisory control. In *2009 European Control Conference (ECC)*, pages 2097–2102, 2009.

[20] P. J. W. Koelewijn and R. Tóth. Scheduling dimension reduction of lpv models - a deep neural network approach. In *2020 American Control Conference (ACC)*, pages 1111–1117, 2020.

[21] A. Kwiatkowski and H. Werner. Pca-based parameter set mappings for lpv models with fewer parameters and less overbounding. *IEEE Transactions on Control Systems Technology*, 16(4):781–788, 2008.

[22] Fabien Lescher, Jing Zhao, and Pierre Borne. Switching lpv controllers for a variable speed pitch regulated wind turbine. *International Journal of Computers, Communications Control*, 1:1334 – 1340, 11 2006.

[23] Panshuo Li, Anh-Tu Nguyen, Haiping Du, Yan Wang, and Hui Zhang. Polytopic lpv approaches for intelligent automotive systems: State of the art and future challenges. *Mechanical Systems and Signal Processing*, 161:107931, 2021.

[24] B. Lu and F. Wu. Switching lpv control designs using multiple parameter-dependent lyapunov functions. *Automatica*, 40:1973–1980, 11 2004.

[25] H. Niemann. Dual youla parameterisation. *IEE Proceedings - Control Theory and Applications*, 150(5):493–, Sep. 2003.

[26] Andy Packard. Gain scheduling via linear fractional transformations. *Systems Control Letters*, 22(2):79–92, 1994.

[27] M. Postma and R. Nagamune. Air-fuel ratio control of spark ignition engines using a switching lpv controller. *IEEE Transactions on Control Systems Technology*, 20(5):1175–1187, 2012.

[28] Shen Qu, Tianyi He, and Guoming Zhu. Engine egr valve modeling and switched lpv control considering nonlinear dry friction. *IEEE/ASME Transactions on Mechatronics*, PP:1–1, 03 2020.

[29] B. Rasmussen and Y. Chang. Stable controller interpolation and controller switching for lpv systems. *Journal of Dynamic Systems Measurement and Control-transactions of The Asme - J DYN SYST MEAS CONTR*, 132, 01 2010.

[30] Rajamani Ravi, Krishan M Nagpal, and Pramod P Khargonekar. $\mathcal{H}_\infty$ control of linear time-varying systems: A state-space approach. *SIAM journal on control and optimization*, 29(6):1394–1413, 1991.

[31] F. R. P. Safaei, J. Hespanha, and Gregory Stewart. On controller initialization in multivariable switching systems. *Automatica*, 48:3157–3165, 2012.

[32] T. Tay, J. Moore, and I. Mareels. *High performance control*. Springer Science & Business Media, 1997.

[33] Tianyi He, Guoming G. Zhu, Sean Shan-Min Swei, and Weihua Su. Simultaneous design of smooth switching state-feedback lpv control. In *Annual American Control Conference (ACC)*, pages 3368–3373, 2018.

[34] F. Wu. *Control of linear parameter varying systems*. PhD thesis, University of California at Berkeley, 1995.

[35] Fen Wu, Xin Yang, Andy Packard, and Greg Becker. Induced l2-norm control for lpv systems with bounded parameter variation rates. *International Journal of Robust and Nonlinear Control*, 6:983–998, 1996.

[36] W. Xie and T. Eisaka. Design of lpv control systems based on youla parameterisation. *IEE Proceedings - Control Theory and Applications*, 151(4):465–472, July 2004.

[37] P. Zhao and R. Nagamune. Switching lpv controller design under uncertain scheduling parameters. *Automatica*, 76:243–250, 2017.

[38] Pan Zhao and Ryozo Nagamune. Optimal switching surface design for state-feedback switching lpv control. In *2015 American Control Conference (ACC)*, pages 817–822, 2015.

A Proof of Lemma 2.1

PROOF. Consider an upper triangular matrix:

$$A(\rho) = \begin{bmatrix} A_{11}(\rho) & A_{12}(\rho) \\ 0 & A_{22}(\rho) \end{bmatrix} \tag{A.1}$$

According to the assumption, there exists bounded positive definite matrix functions $X_1(\rho)$ and $X_2(\rho)$, positive real numbers α_1 and α_2, satisfying the following inequalities [30]:

$$\begin{aligned} \dot{X}_1(\rho) + X_1(\rho)A_{11}(\rho) + A_{11}^T(\rho)X_1(\rho) \le -\alpha_1 I \\ -\alpha_2 I \le \dot{X}_2(\rho) + X_2(\rho)A_{22}(\rho) + A_{22}^T(\rho)X_2(\rho) < 0 \end{aligned} \tag{A.2}$$

Since the off-diagonal matrix $A_{12}(\rho)$ is assumed to be bounded, there exists a positive real number α_3 satisfying

$$X_1(\rho)A_{12}(\rho) \le \alpha_3 I \tag{A.3}$$

$A(\rho)$ is said to be exponentially stable if there exists a positive definite matrix function $X(\rho)$ such that

$$\pi = \dot{X}(\rho) + X(\rho)A(\rho) + A^T(\rho)X(\rho) < 0 \tag{A.4}$$

Choose

$$X(\rho) = \begin{bmatrix} X_1(\rho) & 0 \\ 0 & \lambda X_2(\rho) \end{bmatrix}$$

Then,

$$\pi = \begin{bmatrix} \dot{X}_1(\rho) + X_1(\rho)A_{11}(\rho) + A_{11}^T(\rho)X_1(\rho) & X_1(\rho)A_{12}(\rho) \\ A_{12}^T(\rho)X_1(\rho) & \lambda\big(\dot{X}_2(\rho) + X_2(\rho)A_{22}(\rho) + A_{22}^T(\rho)X_2(\rho)\big) \end{bmatrix}$$

Next, let us find a positive real number $\lambda > 0$ which satisfies (A.4). Using Schur complement, inequality (A.4) is equivalent to the following two inequalities:

$$\begin{aligned} \pi(2,2) < 0 \\ \pi = \pi(1,1) - \pi(1,2)\pi(2,2)^{-1}\pi(2,1) < 0 \end{aligned} \tag{A.5}$$

The first inequality holds for any $\lambda > 0$ (from (A.2)). Considering (A.2) and (A.3) in (A.5), then

$$\pi \le -\alpha_1 I + \lambda^{-1}\alpha_2\pi(1,2)\pi(2,1) \le -\alpha_1 I + \lambda^{-1}\alpha_2\alpha_3^2 I \tag{A.6}$$

Therefore, $\pi < 0$ for any $\lambda > 0$ satisfying $\alpha_2\alpha_3^2/\lambda < \alpha_1$. A similar proof could be deduced for the lower triangular matrices.